

High efficiency amorphous and nanocrystalline silicon solar cells

Baojie Yan*, Guozhen Yue, Xixiang Xu, Jeffrey Yang, and Subhendu Guha

United Solar Ovonic LLC, 1100 West Maple Road, Troy, Michigan, USA

Received 7 August 2009, revised 5 November 2009, accepted 9 November 2009

Published online 19 January 2010

PACS 52.80.Pi, 61.43.Dq, 71.23.Cq, 73.63.Bd, 81.07.Bc, 84.60.Jt

* Corresponding author: e-mail byan@uni-solar.com, Phone: +1-248-519-5304, Fax: +1-248-362-4442

This paper reviews our progress of using nc-Si:H as a low bandgap absorber material to substitute for a-SiGe:H alloys in multi-junction solar cells. We have focused on three topics: (1) high deposition rate, (2) large area uniformity of thickness and material properties, (3) high solar cell and module efficiencies. Initially, we investigated various deposition methods, including RF, VHF, and microwave glow discharges. After several years of systematic studies, we have been convinced that VHF glow discharge is an applicable method to attain high rate and large-area uniform nc-Si:H depositions. We also studied the stability of nc-Si:H solar cells and observed various metastability phenomena in nc-Si:H solar cells. We have reported an initial active-area cell efficiency of 15.4% using an a-Si:H/a-SiGe:H/nc-Si:H triple-junction structure. Subsequently, we have increased the deposition rates to around 1.0–1.5 nm/s and

achieved an initial active-area efficiency of 13.4% using an a-Si:H/nc-Si:H/nc-Si:H triple-junction structure. Recently, a stable total-area efficiency of 12.5% was measured at NREL on our a-Si:H/nc-Si:H/nc-Si:H triple-junction solar cell. We have also developed large-area VHF deposition systems and demonstrated encouraging module efficiencies using a-Si:H/nc-Si:H/nc-Si:H triple-junction structures. Initial and stable aperture-area (400 cm²) efficiencies of 11.0 and 10.1% have been achieved with fully encapsulated modules with a-Si:H/nc-Si:H/nc-Si:H triple-junction structures. In this paper, various aspects of nc-Si:H solar cells are discussed, including the material structures, device design, light trapping, metastability, high efficiency solar cell optimization, and large-area deposition.

© 2010 WILEY-VCH Verlag GmbH & Co. KGaA, Weinheim

1 Introduction Hydrogenated amorphous silicon (a-Si:H) and silicon germanium alloy (a-SiGe:H) have been widely used as the intrinsic layers in thin film solar cells. The efficiency of a-Si:H based solar cells had been steadily increased in the 1990s and reached a record stable active-area efficiency of 13% in 1997 [1]. Since then, no breakthrough in the solar cell efficiency has been made with a-Si:H and a-SiGe:H multi-junction solar cells. It has probably reached the practical limit of a-Si:H and a-SiGe:H based solar cells. The main limiting factor is the high defect density in a-SiGe:H, where the defect density increases with germanium content. In the last decade, major focus at United Solar has been on transferring the a-Si:H/a-SiGe:H/a-SiGe:H triple-junction solar cell structure into large volume roll-to-roll deposition systems [2, 3]. Currently, our production capacity is 180 MW/year.

Compared to other solar cell technologies, the major drawback of a-Si:H based solar cells is low efficiency. Currently, most a-Si:H based solar panels on the market have

stable aperture area efficiencies in the range of 5.0–8.5%, with United Solar's triple-junction solar modules at the high end. In order to improve the solar cell efficiency further, new materials with a low defect density and good transport properties are needed, especially for the low bandgap absorbers as the intrinsic layer of bottom cell in multi-junction structures. Hydrogenated nanocrystalline silicon (nc-Si:H), a potential substitute for a-SiGe:H, has been widely studied in the last 15 years [4–10]. After the first report in 1994 [4], many groups around the world have turned their focus on nc-Si:H solar cells. Compared to a-SiGe:H, nc-Si:H has two advantages: one is high photocurrent density, especially in the red response, and another is reduced light-induced degradation in the solar cell efficiency. A major disadvantage of nc-Si:H cells is that it requires a thicker intrinsic layer. Because of the indirect bandgap in the crystallites, the absorption coefficients of nc-Si:H are much lower than a-SiGe:H; a thick nc-Si:H of >1 μm is normally required for high efficiency solar cells. Therefore, high

deposition rate is essential for mass production of a-Si:H and nc-Si:H based solar products. In order to reach high deposition rates without compromising the material quality, new deposition methods are needed. Over the years, many attempts have been made including very high frequency (VHF) glow discharge [4–10], microwave glow discharge [6, 11, 12], and hot wire chemical vapor deposition (Hot Wire CVD) [13]. Compared to other deposition techniques, VHF is the most promising technique for high rate nc-Si:H depositions. However, the increased frequency in VHF systems causes a great challenge in the thickness and material property uniformity, especially in the high pressure, high power, and small gap-distance regime. Although many engineering approaches have improved the uniformity [14, 15], there are still many challenges to obtain uniform large-area nc-Si:H deposition with VHF. United Solar has worked on a-Si:H and nc-Si:H based solar cells in the last several years. We have mainly focused on three aspects: high rate deposition, large-area uniformity, and high efficiency. We have made significant progress in all three areas. In this paper, we review our achievements and current status. We also present our perspective for future directions.

2 Deposition and optimization of nc-Si:H materials and solar cells In order to make a-Si:H and nc-Si:H multi-junction solar cell structure a viable technology for next generation thin film silicon solar cells, United Solar has taken a stage-gate approach, including demonstration of high efficiency small area solar cells, high rate deposition, large-area uniformity, and finally roll-to-roll continuous deposition. Currently, we focus mainly on small area solar cells and large area modules. Below, we summarize the knowledge we have learned over the years.

2.1 High rate nc-Si:H deposition with various methods We have tried three techniques for the nc-Si:H deposition [6]. In the early stages, we used conventional RF glow discharge at a low rate of ~ 0.1 nm/s for high efficiency solar cells. We have demonstrated an initial active-area efficiency of 13.0% in an a-Si:H/nc-Si:H double-junction solar cell at the low rate [6]. In order to increase the deposition rate, we have used the approach of high pressure and high power using RF glow discharge, with which we reached the deposition rates of 0.3–0.5 nm/s and demonstrated an initial active-area efficiency of 12.4% with an a-Si:H/nc-Si:H double-junction structure. We used modified VHF (MVHF) and microwave glow discharge for high rate depositions. With microwave, we reached a deposition rate of 3–4 nm/s and showed an initial active-area efficiency of $\sim 5\%$ with a single-junction nc-Si:H solar cell [6]. However, we faced the problem of poor nc-Si:H material quality with randomized crystalline orientations instead of (220) preferential orientation. In recent years, we have mainly worked on MVHF deposition at high rates. Currently, the nc-Si:H deposition rates are in the range of 1.0–1.5 nm/s. With these deposition rates, the total deposition time of an a-Si:H/nc-Si:H/nc-Si:H

triple-junction solar cell is close to the total deposition time of an a-Si:H/a-SiGe:H/a-SiGe:H triple-junction solar cell in the manufacturing lines. By optimizing the deposition parameters, we are increasing the nc-Si:H deposition rates further.

2.2 nc-Si:H material structure and optimization nc-Si:H material is a mixture of nanometer-sized grains and amorphous tissues [5]. The carrier transport is mainly through the crystalline paths, where the carrier mobility is much higher. This allows the solar cells to be thick enough for high photocurrent density. In addition, the amorphous phase in nc-Si:H absorbs the short wavelength light more efficiently than c-Si. Therefore, nc-Si:H has the advantage in the optical absorption and can be used as intrinsic layer with a thickness much smaller than c-Si solar cells. However, the nature of indirect bandgap in crystallites leads to a relatively small absorption in the long wavelength, which requires at least 1–2 μm of intrinsic layer in nc-Si:H solar cells. For nc-Si:H deposition, a phenomenon called crystalline volume evolution occurs, where the crystalline volume fraction increases with the nc-Si:H thickness. An example is given in Fig. 1 [16], where the upper plot is a Raman spectrum from a nc-Si:H solar cell and the lower one is the crystalline volume fraction estimated from decomposition of the Raman spectra for cells with different intrinsic layer thicknesses. It clearly shows that the crystalline volume fraction increases with the film thickness. Such an increase of crystalline volume fraction causes poor nc-Si:H solar cell performance. To resolve the nanocrystalline evolution issue

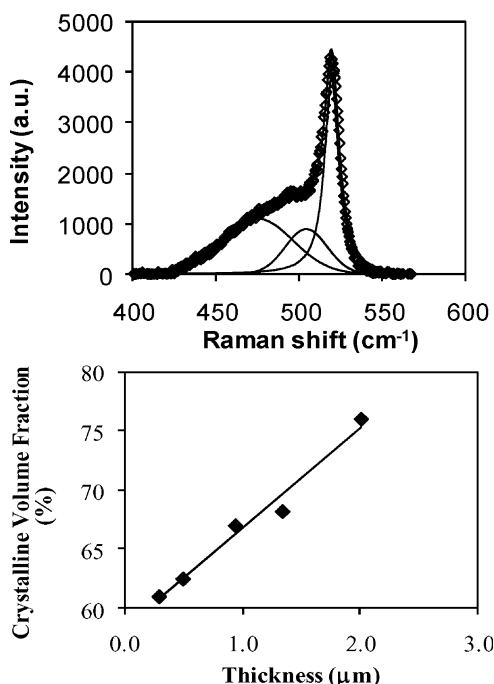


Figure 1 (upper) Raman spectrum of a nc-Si:H solar cell with three components of the decomposition and (lower) the crystalline volume fraction versus cell thickness.

in nc-Si:H solar cells, we have developed a hydrogen dilution profiling technique to control the crystallinity evolution along the growth direction [16]. Because the amorphous to nanocrystalline transition and the crystallinity depend on the hydrogen dilution during the deposition, one can enhance the nanocrystalline formation using very high hydrogen dilution during the initial deposition and suppress the increase of crystallinity by dynamically reducing the hydrogen dilution during the deposition. Experimental results showed that a proper hydrogen dilution profile can effectively control the nanocrystalline evolution as shown in Fig. 2, where the Raman spectra of three nc-Si:H samples with different thicknesses are very similar. We found that a proper hydrogen dilution profiling improves all three J - V characteristic parameters: J_{sc} , V_{oc} , and FF [16]. Currently, our best nc-Si:H solar cells have slightly inversed crystallinity distribution as shown in Fig. 3, where the crystallinity is higher in the bottom region (near the n/i interface) than in the top region (near the i/p interface) [17].

Another issue in nc-Si:H solar cells is the ambient degradation without intentional light soaking, which was caused by high porosity in the material [18]. A porous structure in unoptimized nc-Si:H allowed impurities to diffuse into the material and degrade the cell performance. In some cases, the ambient degradation was so severe that it was readily observed even in an a-Si:H/nc-Si:H double-junction cell, where even the top a-Si:H cell could not block the impurity diffusion. The porous structure of the interface nc-Si:H caused microcracks of the a-Si:H top cell and degraded the a-Si:H/nc-Si:H double-junction cell. SIMS analyses showed an increase of impurity contents in the nc-Si:H bottom cell in the a-Si:H/nc-Si:H double-junction structure. We investigated the deposition parameters and successfully reduced the porosity in the nc-Si:H and improved the cell

performance, where hydrogen dilution profiling plays an important role. It has been reported that nc-Si:H materials made under the conditions close to the nanocrystalline to amorphous transition have a compact structure and the corresponding solar cells showed high efficiencies [19]. This phenomenon implies that nc-Si:H solar cells with a high crystalline volume fraction normally contain a high defect density, presumably resulting from poor grain boundary passivation and post-oxidation through the porous structure. Because of the crystalline evolution, it is difficult to make the crystalline volume fraction close the transition region throughout the entire thickness without hydrogen dilution profiling. Therefore, a proper hydrogen dilution profiling can reduce the crystallinity in the top region of the intrinsic layer, which makes the material more compact and reduces the possibility of post-deposition impurity diffusion.

2.3 Single-junction nc-Si:H solar cell structure

The structure of nc-Si:H solar cells is more complex than a-Si:H solar cells [20]. For a nc-Si:H single-junction solar cell, an a-Si:H buffer layer and a seed layer are inserted at the n/i interface, and another a-Si:H buffer layer at the i/p interface. The n/i buffer layer consists an a-Si:H buffer layer, which is used to reduce phosphorous incorporation into the nc-Si:H intrinsic layer, and a seed layer made with very high hydrogen dilution to promote the nucleation of the nc-Si:H intrinsic layer and remove the amorphous incubation layer. As shown in Fig. 3, no a-Si:H incubation layer is observed in the actual solar cell prepared in our laboratory. The second buffer layer at the i/p junction is an a-Si:H layer, which is designed to reduce the shunt current and improve the open-circuit voltage (V_{oc}). Although the optimization of each layer is important for nc-Si:H solar cell performance, the i/p buffer layer is critical for the solar cell performance.

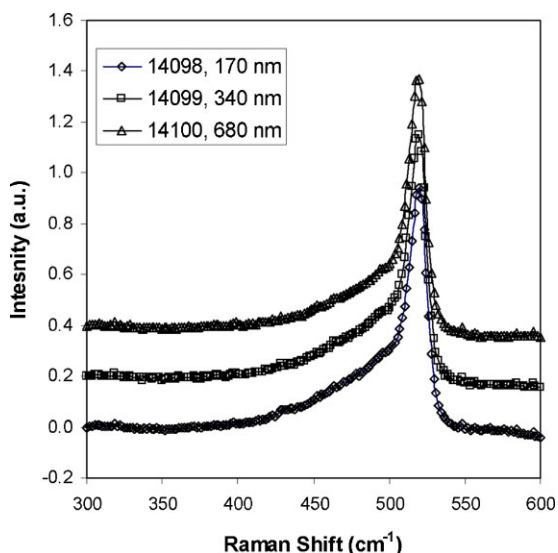


Figure 2 Raman spectra of nc-Si:H layers made with a proper hydrogen dilution profiling. The three samples are with different thicknesses, but a similar crystallinity.

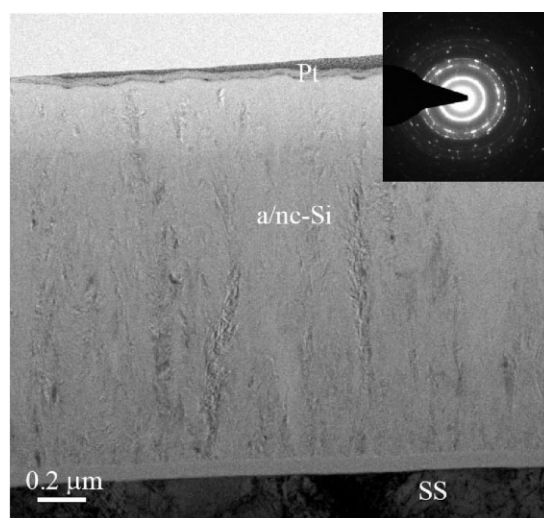


Figure 3 An X-TEM image of nc-Si:H solar cell on SS substrate. Hydrogen profiling is used to create a slightly inversed nanocrystalline distribution.

As reported previously [20], a thin a-Si:H *i/p* buffer layer cannot reduce the shunt current which causes poor V_{oc} and FF. If the a-Si:H *i/p* buffer layer is too thick, the carriers cannot be injected into the intrinsic layer efficiently. It causes that the dark $J-V$ cannot turn on properly, and the dark and light $J-V$ curves crossover. As a result, a poor FF is observed. The thickness of the a-Si:H *i/p* buffer layer can be experimentally optimized.

2.4 Light trapping for nc-Si:H solar cells In high efficiency nc-Si:H solar cells, light trapping plays a significant role in enhancing the photocurrent. Except for the conventional randomized textures for light scattering, many new light trapping approaches for nc-Si:H solar cells have been proposed and studied, such as periodic grating structures, photonic back reflectors, and metal nanoparticles. We found that all these new approaches have not demonstrated a J_{sc} higher than what has been achieved by randomized Ag/ZnO back reflectors at United Solar. By optimizing the Ag and ZnO textures, we have demonstrated a photocurrent enhancement of 60–75% in nc-Si:H solar cells [21]. We have achieved the highest J_{sc} of 29.2 mA/cm² with a nc-Si:H single-junction solar cell with a 2.5 μ m thick nc-Si:H intrinsic layer deposited at 1.0–1.5 nm/s. Figure 4 shows the QE curve of the nc-Si:H solar cell with the comparison of theoretical limitation calculated by E. A. Schiff (private communication) based on the “maximum optical enhancement” of $4n^2$ (n is the refractive index of silicon). One can see that we are approaching the practical limit of light trapping in nc-Si:H solar cells using randomized back reflectors. In order to enhance the light trapping further, new approaches such as periodic gratings, photonic structures, and plasmonic light scattering may be needed. However, one has to prove that

the $4n^2$ limitation could be exceeded with new light trapping approaches.

2.5 Stability of nc-Si:H single-junction and a-Si:H/nc-Si:H based multi-junction solar cells

nc-Si:H solar cells have been found to be more stable than a-Si:H and a-SiGe:H solar cells [4, 5]. However, because of the mixed-phase nature, where nc-Si:H contains nanocrystallites, grain boundaries, and amorphous tissues, the stability of nc-Si:H solar cells is more complicated than a-Si:H solar cells. United Solar has systematically studied the stability of nc-Si:H solar cells [22–24]. The observations are summarized below. First, light-induced degradation has been observed in many nc-Si:H solar cells [22]. However, the light-induced degradation only occurs with photon-energy greater than the crystalline silicon bandgap. No light-induced degradation is observed using red light, which is only absorbed in the nanocrystalline phase. Second, no forward current induced degradation has been observed [22]. The explanation is that the injected carriers under a forward bias only transport in the crystalline phase, where no metastable defects are created. These two observations suggested that the light-induced defect generations happen in the amorphous tissues or the grain boundaries. Third, the light-induced degradation is strongly enhanced by a reverse bias [23, 24], which is very puzzling and opposite to a-Si:H solar cells. In a-Si:H and a-SiGe:H solar cells, light-induced degradation is suppressed by a reverse electrical bias because the bias increases the collection of photo-carriers and reduces the recombination that is the driving force for defect generation. We proposed an explanation for the reverse bias enhanced light-induced degradation in nc-Si:H solar cells. We believe that a reverse bias results in an accumulation of photo-carriers in the grain boundaries, where the recombination enhances the light-induced defect generation. This explanation is supported by a recent photoluminescence study [25].

Although the majority of nc-Si:H solar cells show some degree of metastability, the overall light-induced degradation in nc-Si:H solar cells is much smaller than in a-Si:H and a-SiGe:H solar cells. Therefore, using a nc-Si:H intrinsic layer in the bottom and/or middle cells in multi-junction structures can efficiently reduce the light-induced degradation. For example, the light-induced degradation in a-Si:H/nc-Si:H/nc-Si:H triple-junction solar cells is normally in the range of 3–5%, which is significantly lower than 10–15% in a-Si:H/a-SiGe:H/a-SiGe:H structures. The light-induced degradation in a-Si:H/nc-Si:H double-junction solar cells could be high because of the thick a-Si:H top cell. A semi-transparent inter-reflection layer has been proposed to decrease the top cell thickness and reduce light induced degradation.

2.6 High efficiency nc-Si:H single-junction and multi-junction solar cells

Combining high quality nc-Si:H materials, optimized solar cell design, and improved Ag/ZnO back reflectors, we have achieved an initial active-area solar cell efficiency of 9.5%; the $J-V$ and QE curves are

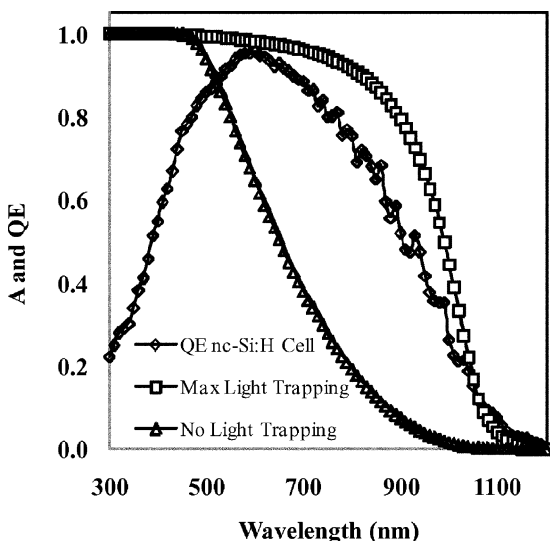


Figure 4 QE curve of a nc-Si:H solar cell on Ag/ZnO back reflector. The triangles and squares are the calculated absorbance (A) spectra with one path and $4n^2$ paths, respectively.

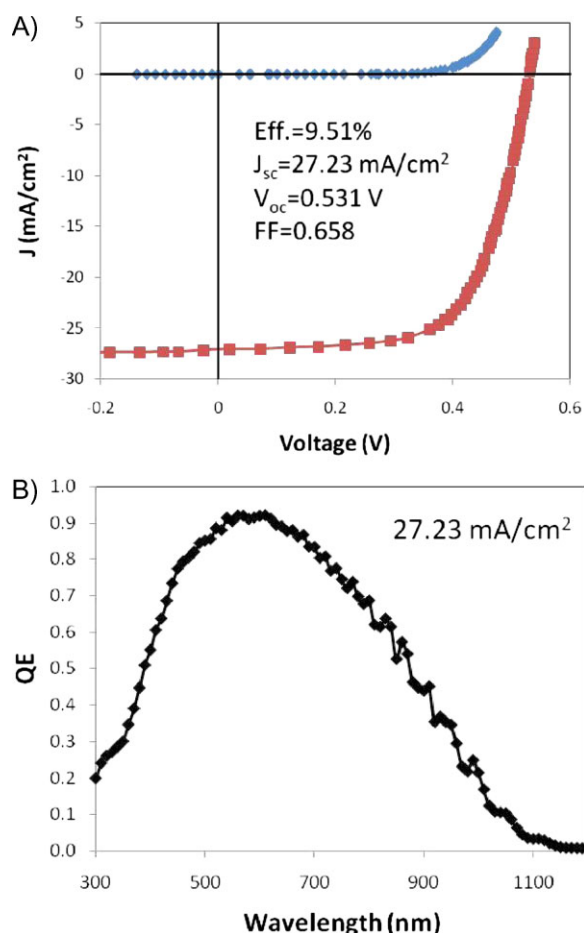


Figure 5 (online color at: www.pss-a.com) (A) J - V characteristics and (B) QE curve of a nc-Si:H single-junction solar cell made with MVHF at a high rate.

shown in Fig. 5 [21]. Using the optimized a-Si:H, a-SiGe:H, and nc-Si:H component cells, we have investigated various multi-junction structures such as a-Si:H/nc-Si:H double-junction, a-Si:H/a-SiGe:H/nc-Si:H triple-junction, and a-Si:H/nc-Si:H/nc-Si:H triple-junction. The highest initial active-area efficiency is 15.4% [26], which was achieved using an a-Si:H/a-SiGe:H/nc-Si:H triple-junction structure. However, the light induced degradation in such solar cells is high. Recently, we have improved the triple-junction solar cell efficiency by using an a-Si:H/nc-Si:H/nc-Si:H triple-junction structure. The light-induced degradation has been reduced to around 3–5%. With this cell structure, we have

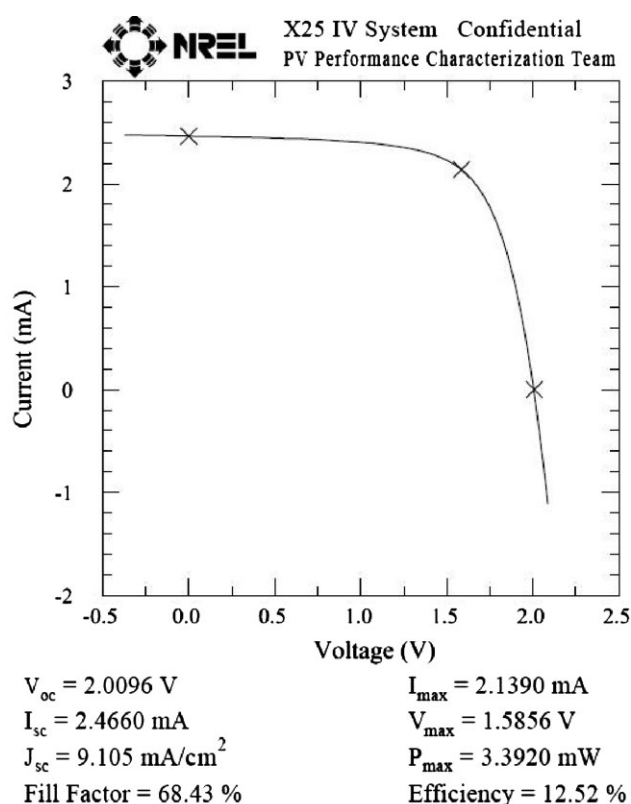


Figure 6 J - V characteristics of an a-Si:H/nc-Si:H/nc-Si:H triple-junction cell with a stable total-area efficiency of 12.5%.

made a new high stable total-area efficiency of 12.5% as measured by the National Renewable Energy Laboratory. Figure 6 shows the J - V characteristics of the highest stable total-area efficiency triple-junction solar cell, where the nc-Si:H layers were deposited with MVHF at 1.0–1.5 nm/s.

2.7 Large-area deposition of a-Si:H and nc-Si:H multi-junction solar cells We initially tested a-Si:H/nc-Si:H double-junction solar cells using a large-area batch machine with RF glow discharge at a deposition rate of ~ 0.5 nm/s. Initial and stable aperture-area efficiencies of 10.5 and 9.5% were achieved over 420 cm² [27]. Recently, we have investigated large area VHF deposition systems [28]. With the knowledge learned from the small-area nc-Si:H solar cell optimization, we have made a-Si:H/nc-Si:H double-junction and a-Si:H/nc-Si:H/nc-Si:H triple-junction solar cells at high deposition rates (>1.0 nm/s).

Table 1 Initial J - V characteristics of large-area encapsulated nc-Si:H based multi-junction solar cells made using MVHF plasma deposition. The aperture area is 400 cm².

cell structure	cell #	V_{oc} (V)	J_{sc} (mA/cm ²)	FF	P_{max} (W)	eff. (%)
a-Si:H/nc-Si:H double-junction	14 333	1.38	11.5	0.64	4.07	10.2
	14 334	1.41	11.5	0.64	4.25	10.6
a-Si:H/nc-Si:H/nc-Si:H triple-junction	15 287	1.85	8.2	0.72	4.36	10.9
	15 297	1.87	8.4	0.70	4.38	11.0

Table 1 lists examples of our current large-area cell performance, where the solar cells were encapsulated using a process similar to our production lines. The highest initial aperture area efficiency of a-Si:H/nc-Si:H/nc-Si:H triple-junction cells is 11.0%, which is slightly higher than that of a-Si:H/nc-Si:H double-junction solar cells. However, the light induced degradation is significantly different. For double-junction solar cells, the light-induced degradation is ~15%, while it is less than 5% for triple-junction solar cells. With the triple-junction structure, we have achieved stable aperture-area (400 cm²) cell efficiency of ~10.1% (10.5% of initial efficiency from this cell). Further improvements in the cell efficiency and large area uniformity are in progress.

3 Future perspective of thin film silicon solar cells United Solar has been manufacturing multi-junction solar modules since 1986. From a pilot plant production of ~600 kW in 1986, it has emerged as the largest manufacturer of solar laminates having an annual production capacity of 180 MW. The spectrum splitting a-Si:H/a-SiGe:H/a-SiGe:H triple-junction cell structure is being used in all the current manufacturing plants. For next generation of silicon thin film solar panel product, a-Si:H and nc-Si:H based solar cell structure is definitely a good candidate. However, before pursuing large-scale deposition systems, the technical issues such as high conversion efficiency, high deposition rate, large-area deposition uniformity, manufacturing capability, and manufacturing cost should be further studied. Currently, we are focusing on these issues.

4 Summary We have reviewed the issues related to nc-Si:H solar cells and the approaches of resolving these issues. From a material structures point of view, nanocrystalline evolution is a critical problem for high efficiency solar cells. It causes poor nc-Si:H quality and potential ambient degradation. This issue can be resolved by optimizing the deposition parameters, especially using a proper hydrogen dilution profiling. The nc-Si:H solar cell structure is normally more complicated than a-Si:H solar cells. The interface buffer layers are critical for high efficiency solar cells. Light trapping is a necessary element for high efficiency nc-Si:H solar cells. At United Solar, advanced Ag/ZnO back reflectors have been developed. The light enhancement is approaching the practical achievable limitation. We have demonstrated high efficiency nc-Si:H single-junction and multi-junction solar cells. Currently, we are still focusing on the three major tasks of high efficiency, high deposition rate, and large-area uniformity of a-Si:H and nc-Si:H based solar cells. We believe that with the improved understanding of nc-Si:H material properties and solar cell design, we shall be able to resolve the issues and introduce a-Si:H and nc-Si:H based multi-junction solar cells in the manufacturing lines.

Acknowledgements We thank the entire Research and Development Department at United Solar Ovonic for their contribution and great teamwork. This work was supported by US DOE under SAI Program contract no. DE-FC36-07 GO 17053.

References

- [1] J. Yang, A. Banerjee, and S. Guha, *Appl. Phys. Lett.* **70**, 2975 (1997).
- [2] J. Yang, A. Banerjee, and S. Guha, *Sol. Energy Mater. Sol. Cells* **78**, 597 (2003).
- [3] M. Izu and T. Ellison, *Sol. Energy Mater. Sol. Cells* **78**, 613 (2003).
- [4] J. Meier, R. Flückiger, H. Keppner, and A. Shah, *Appl. Phys. Lett.* **65**, 860 (1994).
- [5] A. V. Shah, J. Meier, E. Vallat-Sauvain, N. Wyrsh, U. Kroll, C. Droz, and U. Graf, *Sol. Energy Mater. Sol. Cells* **78**, 469 (2003).
- [6] B. Yan, G. Yue, J. Yang, K. Lord, A. Banerjee, and S. Guha, in: *Proceedings of the 3rd World Conference on Photovoltaic Energy Conversion*, Osaka, Japan, 2003, pp. 2773–2777.
- [7] B. Yan, G. Yue, and S. Guha, *Mater. Res. Soc. Symp. Proc.* **989**, 335 (2007).
- [8] S. Fukuda, K. Yamamoto, A. Nakajima, M. Yoshimi, T. Sawada, T. Suezaki, M. Ichikawa, Y. Koi, M. Goto, T. Meguro, T. Matsuda, T. Sasaki, and Y. Tawada, in: *Proceedings of the 21st European PVSEC Conference*, Geramny, 2006, pp. 1535–1538.
- [9] Y. Mai, S. Klein, R. Carius, J. Wolff, A. Lambertz, F. Finger, and X. Geng, *J. Appl. Phys.* **97**, 114913 (2005).
- [10] K. Saito, M. Sano, S. Okabe, S. Sugiyama, and K. Ogawa, *Sol. Energy Mater. Sol. Cells* **86**, 565 (2005).
- [11] H. Jia, H. Shirai, and M. Kondo, *Mater. Res. Soc. Symp.* **910**, 309 (2006).
- [12] L. Löffler, C. Devilee, M. Geusebroek, W. J. Soppe, and H.-J. Muffler, in: *Proceedings of the 21st European PVSEC*, Geramny, 2006, pp. 1597–1600.
- [13] A. H. Mahan, *Sol. Energy Mater. Sol. Cells* **78**, 299 (2003).
- [14] H. Takatsuka, Y. Yamauchi, Y. Takeuchi, M. Fukagawa, K. Kawamura, S. Goya, and A. Takano, in: *Record of the 4th World Conference on Photovoltaic Energy Conversion*, Hawaii, USA, 2006, pp. 2028–2031.
- [15] S. Sheng, Y. Chae, L. Li, J. Su, X. Yang, A. Kadam, D. Tanner, C. Eberspacher, T. Won, S. Choi, and J. White, in: *Proceedings of the 23rd European Photovoltaic Solar Energy Conference*, Geramny, 2008, pp. 2443–2446.
- [16] B. Yan, G. Yue, J. Yang, S. Guha, D. L. Williamson, D. Han, and C.-S. Jiang, *Appl. Phys. Lett.* **85**, 1955 (2004).
- [17] G. Yue, B. Yan, G. Ganguly, J. Yang, S. Guha, and C. W. Teplin, *Appl. Phys. Lett.* **88**, 263507 (2006).
- [18] B. Yan, K. Lord, J. Yang, S. Guha, J. Smeets, and J.-M. Jacquet, *Mater. Res. Soc. Symp. Proc.* **715**, 629 (2002).
- [19] T. Roschek, T. Repmann, J. Müller, B. Rech, and H. Wagner, in: *Proceedings of the 28th IEEE PVSC*, Anchorage, Alaska, USA, 2000, pp. 150–153.
- [20] G. Yue, B. Yan, C. W. Teplin, J. Yang, and S. Guha, *J. Non-Cryst. Solids* **354**, 2440 (2008).

- [21] G. Yue, B. Yan, L. Sivec, J. M. Owens, S. Hu, X. Xu, J. Yang, and S. Guha, in: Proceedings of the 34th IEEE PVSC, Philadelphia, Pennsylvania, USA, 2009, in press.
- [22] B. Yan, B. Yan, G. Yue, J. M. Owens, J. Yang, and S. Guha, Appl. Phys. Lett. **85**, 1925 (2004).
- [23] G. Yue, B. Yan, J. Yang, and S. Guha, Appl. Phys. Lett. **86**, 092103 (2005).
- [24] G. Yue, B. Yan, G. Ganguly, J. Yang, and S. Guha, J. Mater. Soc. **22**, 1128 (2007).
- [25] K. Wang, D. Han, G. Yue, B. Yan, J. Yang, and S. Guha, Appl. Phys. Lett. **95**, 023506 (2009).
- [26] B. Yan, G. Yue, J. Yang, and S. Guha, in: Proceedings of the 33rd IEEE PVSC, San Diego, California, USA, May 2008, Paper No. 257.
- [27] B. Yan, G. Yue, A. Banerjee, J. Yang, and S. Guha, Mater. Res. Soc. Symp. Proc. **808**, 581 (2004).
- [28] X. Xu, T. Su, D. Beglau, S. Ehlert, G. Pietka, D. Bobela, Y. Li, K. Lord, G. Yue, J. Zhang, B. Yan, C. Worrel, K. Beernink, G. DeMaggio, A. Banerjee, J. Yang, and S. Guha, in: Proceedings of the 34th IEEE PVEC, Philadelphia, Pennsylvania, USA, 2009, in press.